

Nocturnal subcanopy flow regimes and missing carbon dioxide

Dean Vickers^{a,*}, James Irvine^b, Jonathan G. Martin^b, Beverly E. Law^b

^a College of Oceanic and Atmospheric Sciences, COAS Admin Bldg 104, Oregon State University, Corvallis, OR 97331-5503, USA

^b College of Forestry, Oregon State University, Corvallis, OR, USA

ARTICLE INFO

Article history:

Received 31 January 2011

Received in revised form 25 August 2011

Accepted 6 September 2011

Keywords:

Nighttime flux problem

Carbon dioxide flux

Carbon dioxide advection

Subcanopy flow

Flux from eddy covariance and chambers

Coupling between above canopy and subcanopy flow

ABSTRACT

Two distinct nocturnal subcanopy flow regimes are observed beneath a tall (16 m) open pine forest canopy. The first is characterized by weaker mixing, stronger stability, westerly downslope flow decoupled from the flow above the canopy and much smaller than expected ecosystem respiration from the eddy flux plus storage measurements compared to estimates based on chambers (missing carbon dioxide). The second regime is characterized by stronger mixing, weaker stability, southerly flow coupled to the flow above the canopy and good agreement between the eddy flux plus storage estimate and the chamber-based estimate of ecosystem respiration. The observations show that the inferred advection terms dominate the carbon dioxide budget in the first regime and are small relative to the eddy flux plus storage terms in the stronger mixing second regime, where the advection is estimated as a residual taking chamber-based measurements of respiration as truth. The friction velocity, standard deviation of vertical velocity, bulk Richardson number, Monin–Obukhov length scale and the subcanopy 3-m wind direction are all good indicators of missing carbon dioxide at this site.

© 2011 Elsevier B.V. All rights reserved.

1. Introduction

One potential source of error with the standard method of estimating the net ecosystem exchange of carbon by summing the eddy flux and storage terms is that it neglects the advection terms in the conservation equation (e.g., Lee, 1998; Finnigan, 1999; Feigenwinter et al., 2004). In most studies reporting long-term carbon budgets, the advection terms are neglected because of the prohibitive cost of instrumentation. In addition, it is not clear that one can measure the advection terms to the required accuracy even with large field efforts (Heinesch et al., 2006; Leuning et al., 2008 and references therein). Also see the special issue of Agricultural and Forest Meteorology, volume 150, May 2010. From our experience, correctly estimating the mean weak vertical motion, required for calculating the vertical advection of CO₂, from a sonic anemometer in the field is very difficult given uncertainty in sonic tilt correction methods (Vickers and Mahrt, 2006). Another problem is that measurements of the small horizontal CO₂ gradient, required to calculate the horizontal advection of CO₂ may be contaminated by the large vertical gradient. While some success has been reported for direct measurements of the advection terms (e.g., Staebler and Fitzjarrald, 2004) and for improved understanding of the forcing in the subcanopy (Staebler and Fitzjarrald, 2005), large uncertainty in such estimates remain.

Advection potentially affects many flux measurement sites because horizontal heterogeneity in either the source-sink distribution (e.g., vegetation type or age class) or the wind field (due to varying terrain or roughness) results in advection of scalars (Lee et al., 2004). Most forest flux tower sites have some degree of heterogeneity in either the vegetation or the topography or both. For example, it has been estimated that only one-third of the CarboEurope flux tower sites are situated in truly homogeneous terrain (Göckede et al., 2008). In addition to advection, the turbulence horizontal flux divergence terms are also neglected; however, the magnitude of these terms is generally thought to be smaller than the advection terms, although additional observations are needed (Staebler and Fitzjarrald, 2004).

The commonly reported signature of the missing CO₂ problem is that the eddy flux plus storage terms under-estimate the expected ecosystem respiration in weak mixing nocturnal conditions, and increase with increasing mixing strength (Gu et al., 2005). The explanation often proposed for the missing CO₂ is the neglected advection of air with lower CO₂ concentration to the tower site in cold air drainage flows associated with the local topography (Sun et al., 1998; Aubinet et al., 2003, 2005; Finnigan and Belcher, 2004; Staebler and Fitzjarrald, 2004; Feigenwinter et al., 2004; Katul et al., 2006; Kominami et al., 2008; Tota et al., 2008).

Ideally, the numerous applied studies that calculate annual sums of carbon fluxes would have sufficient instrumentation and expertise to directly evaluate the advection terms. However this is not the case, and such studies are forced to use less rigorous methods. These methods include filters that discount the

* Corresponding author. Tel.: +1 541 737 5706.

eddy-flux estimates in weak mixing conditions, often defined to be when the friction velocity (u_*) above the canopy is less than some critical value (Goulden et al., 1996; Falge et al., 2001). While the u_* -filter method has been applied to many sites, it has also been widely criticized as not having a strong physical justification. The method is unsatisfying because it does not include direct information on the turbulence or the mean flow in the subcanopy, including whether or not drainage flows even develop.

Here we test whether the turbulence above the canopy and the subcanopy flow patterns are consistent with each other and with missing CO_2 associated with drainage flows. That is, can the characteristics of the above-canopy flow predict the subcanopy flow patterns, and can the subcanopy flow patterns identify those periods with missing CO_2 . An important aspect of the analysis is that the periods with missing CO_2 are identified by comparing the eddy flux plus storage terms (FS) to coincident chamber-based estimates of ecosystem respiration (ER), which depend only on temperature and soil moisture, not characteristics of the flow. Here, ER is taken as truth and differences between ER and FS are related to characteristics of the flow above and below the canopy. ER is based on six automated soil chambers, periodic manual soil respiration measurements, and estimates of foliage and live wood respiration derived from temperature response functions specific to the site. An advantage of this method compared to the standard approach of plotting FS against the friction velocity is that the latter includes the combined influences of temperature and mixing strength, and it is not always clear how to extract the mixing strength effect when the friction velocity and the air temperature are correlated. The approach used here also has the important advantage of being able to identify an advective influence even for those conditions where FS levels off with increasing mixing strength. We are not aware of a previous study incorporating chamber data with this approach to relate missing CO_2 to the subcanopy flow, and the subcanopy flow to the turbulence strength above the canopy.

2. Materials and methods

2.1. Site description

The site is a mature ponderosa pine forest in semi-arid Central Oregon, U.S.A. (44.451 N latitude, 121.558 W longitude, 1255 m elevation) (Schwarz et al., 2004; Irvine et al., 2008). The pine canopy extends from 10 to 16 m above ground level (agl), and the understory consists of scattered 1-m tall shrubs. The leaf area index (LAI) ranges from 3.1 to 3.3 during the growing season and the stand density is 325 trees ha^{-1} .

Although the site is located on a relatively flat saddle region about 500 m across, it is surrounded by complex terrain (Fig. 1). The topography generally rises to the northwest, west and southeast of the tower, falls to the north, south and northeast, and is flat to the southwest and east. The topographic slope strongly depends on the direction and fetch considered (Fig. 2). For the period of record in the summer of 2004, the nocturnal wind direction above and below the canopy is between 180 and 290°, 85% of the time, and the average wind speed is 3.7 m s^{-1} at 30 m agl and 0.37 m s^{-1} at 3 m agl.

2.2. Measurements

Eddy-covariance measurements were collected using a three-dimensional sonic anemometer (model CSAT3, Campbell Scientific Inc., Logan, UT) and an open-path infrared gas analyzer (model LI-7500, LI-COR Inc., Lincoln, NE) at 30 m agl (or about twice the

canopy height). Coincident subcanopy measurements were made using two CSAT3 anemometers at 3 m agl located 10 m away from the main tower to avoid obstructions near the base of the 30-m tower. A tilt correction based on the average wind direction dependence of the tilt angle is applied to the fast-response wind components (Paw U et al., 2000; Feigenwinter et al., 2004). Eddy-covariance fluxes and variances are calculated using a 10-min perturbation timescale and products of perturbations are averaged over 1 h. The primary effect of using a shorter 10-min perturbation timescale for nocturnal fluxes, compared to the commonly used 30-min timescale, is a reduction in the random flux sampling error (Vickers and Mahrt, 2003). We do not discard downward CO_2 fluxes at night to avoid conversion of random error into systematic error (Mahrt, 2010).

Additional measurements include profiles of the mean CO_2 concentration for computing the storage term using a closed-path infrared gas analyzer (model LI-6262, LI-COR Inc.) with inlets at 1, 3, 6, 15 and 30 m agl, and atmospheric temperature profiles measured using platinum resistance thermometers (model HMP45, Vaisala, Oyj, Helsinki, Finland). The storage term is computed using the difference between mean CO_2 concentrations for the half hour before and after the one for which the storage is being estimated, and numerical integration from the surface up to 30 m agl. The 30-min estimates of the storage term are then averaged over 1 h to coincide with the averaging periods used for the soil chamber measurements and the turbulence fluxes.

We employ measurements from an automated soil chamber system based on the design of Crill (1991) (see also Goulden and Crill, 1997) with six chambers with 0.21 m^2 sampling area per chamber (Irvine and Law, 2002). The six chambers were installed 100 m south of the tower in a circle of radius of 10 m. An estimate of ecosystem respiration based on chamber measurements was made by combining high temporal resolution (1-h average) data from the automated soil respiration system (Irvine et al., 2008) with estimates of foliage and live wood respiration derived from temperature response functions specific to ponderosa pine (Law et al., 1999). Extensive periodic manual soil respiration measurements covering an area of several hectares in the estimated footprint of the eddy-covariance fluxes were made using a LI-COR 6400 and a LI-COR 6000-9 soil chamber. The respiration measurements from the automated soil chamber system were corrected for spatial heterogeneity by calibrating them to the manual estimates (Irvine et al., 2008). Litter respiration is included in the soil chamber estimates.

The analysis is focussed on the May–August period of 2004 when the two subcanopy sonic anemometers and the soil chamber system were operational. In addition, decomposition rates of coarse woody debris are not well known over timescales shorter than a year, however, they are most likely to be insignificant during the dry summer months, the available manual chamber estimates of foliage and live wood respiration were collected during the summer and may not be applicable to other seasons, and finally this period captures the seasonal peak in ecosystem respiration (Schwarz et al., 2004). After screening the data for plausibility, small relative random flux sampling error (the standard deviation of the 10-min eddy-flux over the 1-h period divided by the mean 1-h flux) and retaining the 1-h data only when all variables pass the screening for that hour, the entire dataset includes 530 1-hour nocturnal averages.

We also consult subcanopy wind measurements made in August and September of 2003. Five two-dimensional sonic anemometers (Handar model 425A, Vaisala) were deployed in a ring formation on the plateau approximately 100 m from the 30-m flux tower to measure the spatial variability of the mean horizontal wind at 1 m agl. The elevation differences between the Handar sonic locations and the main tower are all less than 4 m.

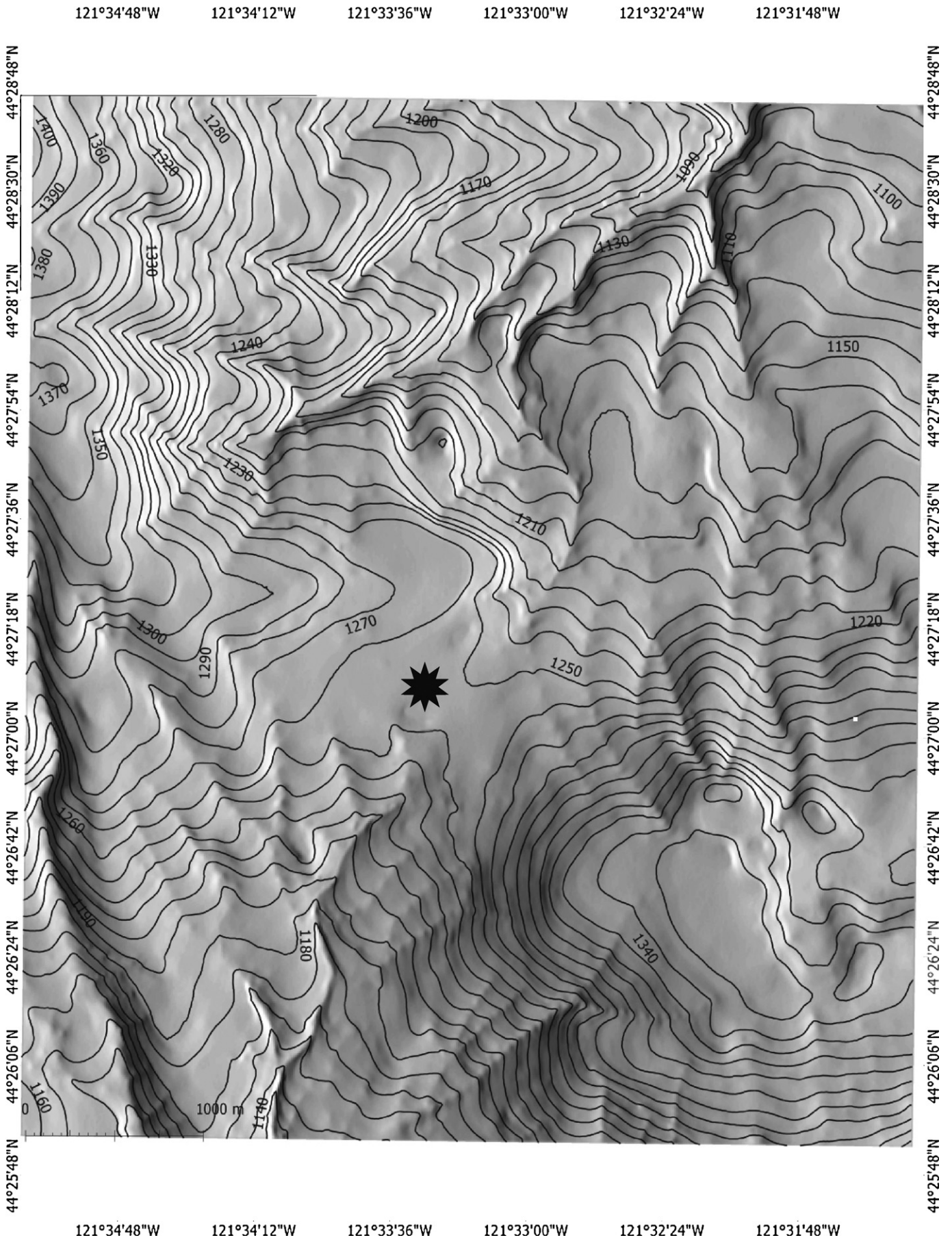


Fig. 1. Topography surrounding the 30-m tower at the mature ponderosa pine site. Contour interval is 10 m. The area shown is approximately 5 × 5 km.

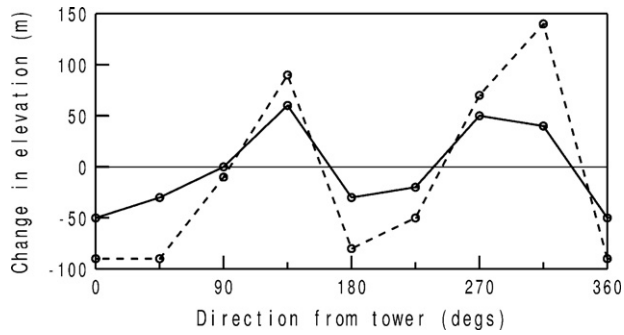


Fig. 2. The change in elevation as a function of direction for distances of 1 km (solid) and 2 km (dash) from the tower.

2.3. Normalized flux plus storage

Instead of the common approach of examining the eddy flux plus storage (FS) as a function of the friction velocity for multiple temperature and perhaps soil moisture classes, we examine a normalized FS (or NFS), which is FS divided by ER, the estimate of ecosystem respiration based on the chamber data,

$$\text{NFS} \equiv \frac{\text{FS}}{\text{ER}} \equiv \frac{\text{eddy flux} + \text{storage method}}{\text{chamber method}}. \quad (1)$$

This normalization was also used by Van Gorsel et al. (2007) in their Fig. 2. This approach has the important advantage of being able to identify a potential advective influence in all conditions, as opposed to the common approach where it is assumed that advection is negligible for mixing stronger than some critical value where FS typically stops increasing with u^* and approaches a constant value that is a function of temperature. For example, with the normalization, if NFS approaches a value different than unity as the mixing strength increases to the largest observed values, we might infer that advection was important even for the cases of strongest mixing. In addition, the normalization improves the statistics because the data do not need to be partitioned into multiple temperature and soil moisture classes. A further benefit is that one avoids the scatter due to variations in temperature within a given temperature class, and also avoids difficulties associated with correlation between temperature and u^* . A disadvantage is the large effort required to obtain high quality continuous chamber-based estimates of ecosystem respiration and correcting for spatial heterogeneity.

Interpretation of variations in NFS with flow conditions relies on ER being an unbiased estimate of ecosystem respiration in all conditions. Based on the detailed analysis of Irvine et al. (2008), there is no known reason why ER would be biased. Over the May–August period, the observed nocturnal 1-h average ER ranges from 3.2 to 6.3 $\mu\text{mol m}^{-2} \text{s}^{-1}$, and generally increases with increasing 3-m air temperature; however, after the onset of the summer dry period in July, the respiration becomes water-limited and is no longer a strong function of temperature.

3. Results and discussion

3.1. Case studies

We first briefly examine individual time series of estimates for ecosystem respiration from the eddy flux plus storage method (FS) and the chamber method (ER) for five different nights (Fig. 3). Cases 1 and 2 are strong wind and strong mixing examples where FS exceeds ER throughout most of the night. One explanation for FS > ER would be horizontal advection of higher CO_2 concentration air to the tower site. Case 3 is a weak wind case where FS is very small compared to ER except right after sunset. Better agreement

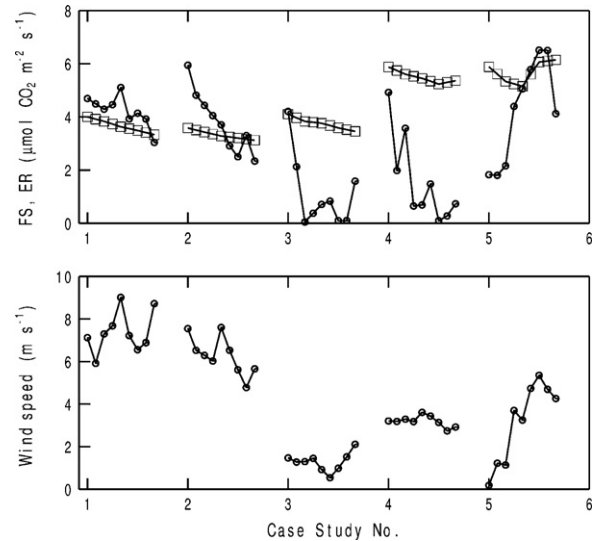


Fig. 3. Nocturnal time series of 1-hourly averaged eddy flux plus storage (FS, dots) and the chamber-based estimate of ecosystem respiration (ER, squares), and the wind speed above the canopy (bottom panel) for five case study nights. Local time varies from 2000 through 0400.

between FS and ER in the early evening was observed by Aubinet et al. (2005) and Van Gorsel et al. (2007). The very small values of FS compared to ER later in the evening may be due to unaccounted for advection, as explored further below. The decrease in ER with time, which is observed on most nights, is associated with cooling during the night. Case 4 is similar to Case 3, although the agreement between early evening FS and ER is not as good.

In Case 5, FS generally increases through the night and the disagreement between FS and ER is largest right after sunset. A plausible explanation is that an early evening drainage flow develops in part due to very weak winds above the canopy, and is then eliminated later in the night by the increase in wind speed (Fig. 3). We speculate that as the drainage flow is eliminated by increased downward mixing of momentum, the relative importance of advection decreases and FS increases towards better agreement with ER. The increasing trend in ER in the latter half of the night is related to an increase in the subcanopy air temperature due to enhanced downward mixing of warmer air associated with increased shear generation of turbulence.

3.2. Missing CO_2

In this section we examine whether the turbulence above the canopy can explain variations in NFS, where values of NFS < 1 indicate missing CO_2 . Plotting NFS against u^* clearly indicates that NFS increases with increasing u^* and then levels off for u^* above a critical value (Fig. 4a). NFS increases by an order of magnitude from about 0.1 to unity with increasing downward momentum flux above the canopy. The missing CO_2 problem affects 70% of the nocturnal flux data, where the critical u^* value is 0.67 m s^{-1} (Fig. 4a) using the 95% rule: the critical value is the smallest u^* class value with an NFS class mean that is greater than or equal to 95% of the average NFS for all larger u^* classes. The average NFS for u^* greater than the critical value is 1.06, and the 95% confidence interval includes unity. The excellent agreement between FS and ER for the strongest mixing conditions lends credence to the hypothesis that advection becomes unimportant relative to FS with stronger mixing conditions.

Using the standard deviation of the vertical velocity (σ_w) instead of the friction velocity, as suggested by Acevedo et al. (2009), yields nearly identical results (Fig. 4b), where 70% of the data is

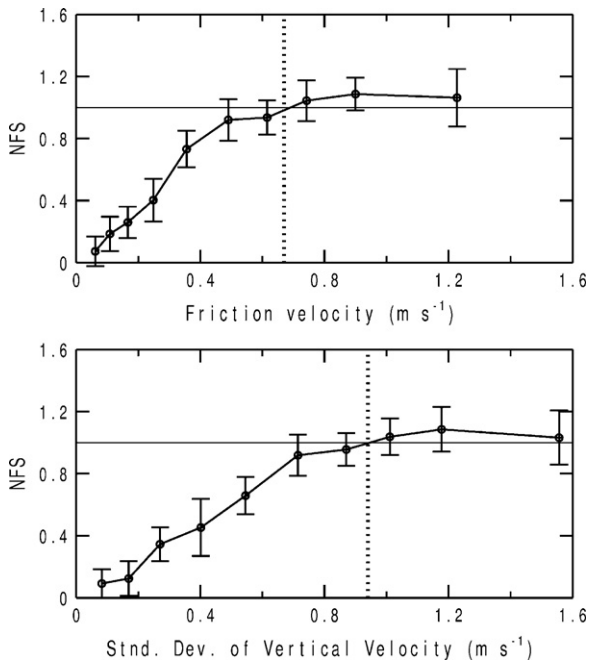


Fig. 4. The normalized eddy flux plus storage (NFS = FS/ER) as a function of the above canopy friction velocity and the standard deviation of vertical velocity. The dashed vertical lines denote the critical values using the 95% rule. Error bars denote the 95% confidence interval. Each of the 10 bins contains 53 1-hour average samples.

flagged and the average NFS for σ_w greater than the critical value of 0.94 m s^{-1} is 1.05. As for u_* , the 95% confidence interval for NFS includes unity for σ_w greater than the critical value.

We now examine the turbulence strength at 3 m agl in the subcanopy. NFS increases with the subcanopy turbulence strength and approaches unity for the strongest turbulence cases (Fig. 5). However, for about one-third of the data consisting of the weakest turbulence periods, there is no significant dependence of NFS on subcanopy turbulence strength. A possible explanation is that

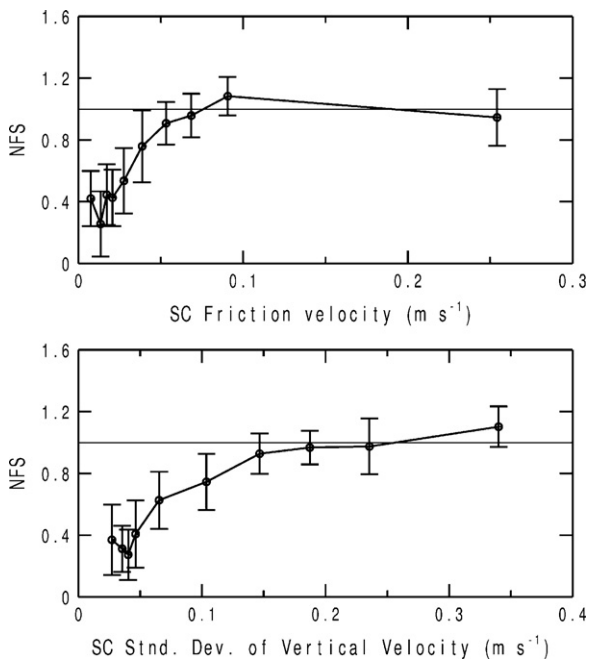


Fig. 5. NFS as a function of the subcanopy (SC) friction velocity and standard deviation of vertical velocity. Error bars denote the 95% confidence interval. Each of the 10 bins contains 53 1-hour average samples.

Table 1

Statistics for different filter variables: none, friction velocity, standard deviation of vertical velocity, bulk Richardson number, stability z/L and the subcanopy wind direction (SC WD). The critical values are found using the 95% rule.

Filter variable	Critical value	Percent data retained	Average NFS of retained data
None	–	100	0.65
u_*	0.67 m s^{-1}	30	1.06
σ_w	0.94 m s^{-1}	30	1.05
R_b	0.025	30	1.04
z/L	0.10	40	1.01
SC WD	226°	60	0.91

the 3-m turbulence measurements are influenced by individual roughness elements (understorey) contributing to scatter in the momentum flux and vertical velocity variance. While both u_* above and below the canopy are useful for identify periods with small NFS, the two estimates of 1-h average u_* are not strongly correlated ($r=0.76$), and the weaker correlation between u_* and σ_w in the subcanopy ($r=0.85$) compared to above the canopy ($r=0.99$) may reflect the problems making representative turbulence measurements in the spatially heterogeneous subcanopy. The above canopy turbulence measurements have no nearby obstructions and may be more representative for describing the general flow conditions. Differences between the estimates of u_* above and below the canopy were not found to be strongly correlated to other features of the flow. As a result, we find no advantage to using the subcanopy turbulence over the above canopy turbulence for the purpose of identifying periods with small NFS. This result may be site-specific.

Using a bulk Richardson number, a stability parameter proportional to the temperature difference between 30 m and 3 m agl divided by the 30-m wind speed squared, also flags 70% of the data and the average NFS for R_b less than the critical value of $R_b = 0.025$ is 1.04. Note that this critical R_b value is based on the R_b -dependence of NFS, and does not refer to the critical Richardson number of classical turbulence theory. Using stability parameter z/L , where L is the Obukhov length scale computed from the above canopy turbulence fluxes of virtual temperature and momentum, flags 60% of the data and the average NFS for z/L less than the critical value of 0.10 is 1.01 (Table 1).

The four indicator variables of mixing strength (u_* , σ_w , R_b and z/L) clearly suggest missing CO_2 in weak mixing conditions but not in strong mixing conditions. A potential physical basis is that nocturnal subcanopy drainage flows are most likely to occur with weak winds, stable stratification and small u_* , when even small surface heterogeneity or small changes in topography can strongly influence local flow patterns near the surface (Mahrt et al., 2001; Staebler and Fitzjarrald, 2005; Belcher et al., 2008). In contrast, strong winds and strong mixing tend to eliminate local flow patterns associated with surface heterogeneity. However, the relationship between the flow above and below the canopy will also depend on the characteristics of the canopy, as reflected in the large range of critical u_* values reported in the literature (Massman and Lee, 2002). In the next section we examine relationships between the turbulence strength above the canopy and the mean flow in the subcanopy.

3.3. Subcanopy mean flow

The dependence of the mean flow at 3 m agl in the subcanopy on the turbulence above the canopy is shown in Fig. 6. With weaker turbulence (or weaker winds) above the canopy, subcanopy flow from the SW-NW develops, and the strength of the flow is inversely proportional to the turbulence strength above the canopy. This decoupling suggests a primary forcing other than stress divergence in the subcanopy, most likely buoyancy forcing and cold air

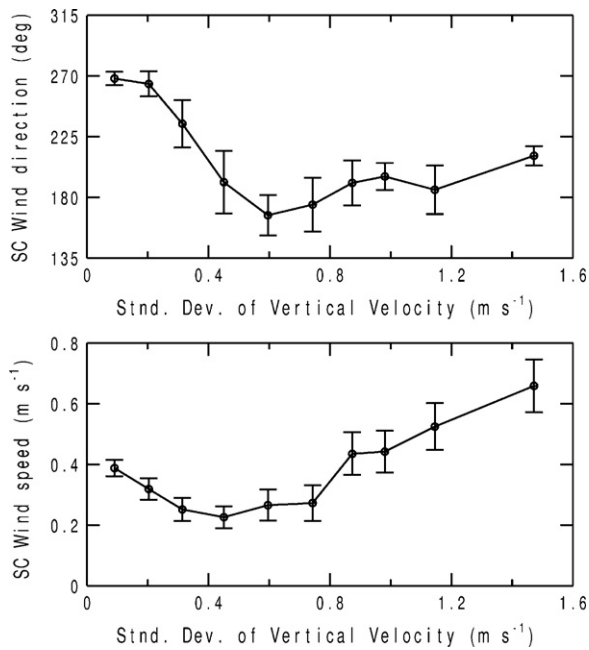


Fig. 6. The subcanopy (SC) wind direction and wind speed as a function of the standard deviation of vertical velocity above the canopy. Error bars denote the 95% confidence interval. Each of the 10 bins contains 53 1-hour average samples.

drainage flow (Staebler and Fitzjarrald, 2005). The very small scatter in the subcanopy wind direction for the cases with the weakest turbulence above the canopy (Fig. 6a) suggests a subcanopy down-slope flow with a narrow range of preferred direction determined by the local topography. In the strongest turbulence (or strongest winds), the subcanopy mean flow is from the SE-SW and the subcanopy wind speed is proportional to the turbulence above the canopy, indicating a coupling between the above canopy and subcanopy flow through the stress divergence, where the subcanopy flow is primarily determined by downward mixing of momentum from above the canopy.

The relationship between the directional shear of the mean wind and the above canopy mixing strength is shown in Fig. 7. In stronger mixing, the average directional shear is near zero, again suggesting that downward mixing of momentum determines the subcanopy flow; however, with weaker mixing, the average directional shear is different from zero and clearly increases with decreasing turbulence strength above the canopy.

Following Staebler and Fitzjarrald (2005) in their Eq. (5), we computed rough estimates of the vertical stress divergence and

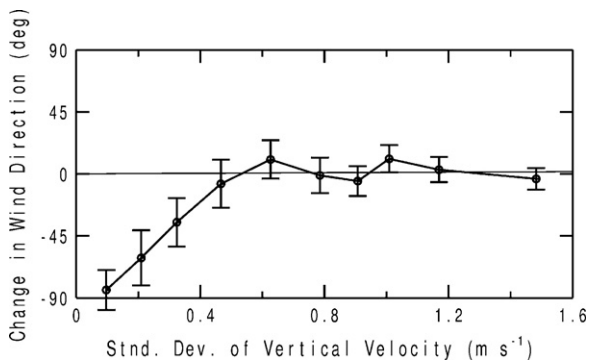


Fig. 7. The change in wind direction (above the canopy minus below the canopy) as a function of the standard deviation of vertical velocity above the canopy. Error bars denote the 95% confidence interval. Each of the 10 bins contains 53 1-hour average samples.

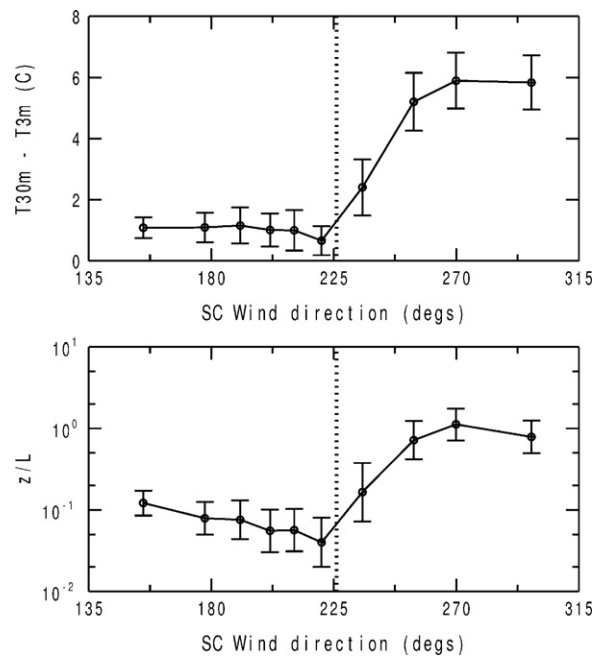


Fig. 8. The vertical temperature difference and the stability parameter of Monin–Obukhov similarity theory, z/L , as a function of the subcanopy (SC) wind direction. The dashed vertical lines denote the critical wind direction based on NFS (Fig. 9). Error bars denote the 95% confidence interval. Each of the 10 bins contains 53 1-hour average samples.

the buoyancy forcing for weak (strong) mixing conditions, defined when the above canopy friction velocity is less than (greater than) the critical value of 0.67 m s^{-1} . To estimate the buoyancy term we used a perturbation potential temperature equal to the vertical temperature difference between 3 and 30 m agl and a terrain slope of 5%. The stress divergence was calculated using the difference in the momentum flux between 3 and 30 m agl. For the weak mixing class, the ratio of the buoyancy term to the stress divergence term averages 3 with a standard deviation of 4, indicating that buoyancy forcing is important and drainage flow is expected. For the strong mixing class, the ratio of the stress divergence term to the buoyancy term is 7 with a standard deviation of 3, indicating that buoyancy forcing is less important and drainage flow is unlikely. These crude estimates are consistent with the decoupled and coupled subcanopy regimes discussed above; however, they are inconclusive for determining the subcanopy flow due to a lack of information on the other terms in the momentum budget equation.

With westerly subcanopy flow, the stratification is much stronger (Fig. 8a). The sharp transition in the temperature profile occurs precisely at the critical value of the subcanopy wind direction based on the wind directional dependence of NFS (Fig. 9). A similar pattern is found for the above canopy stability parameter z/L (Fig. 8b), including the sharp transition from weaker stability in southerly flow to stronger stability in westerly subcanopy flow. The vertical temperature structure and z/L clearly demonstrate two distinct subcanopy flow regimes and support the critical subcanopy wind direction value based on the missing CO_2 .

Here we briefly examine the nocturnal wind measurements from the ring of five Handar two-dimensional sonic anemometers located on the plateau 100 m from the 30-m tower in 2003. The dashed curves in Fig. 10 are for two locations south and south-east of the tower, at the top of the ravine that extends south of the tower (Fig. 1). With weak wind above the canopy, the flow at these locations has a stronger northerly component, possibly due to a shallow drainage flow down the ravine. The solid curves in Fig. 10 are for three locations to the north and west of the tower. At

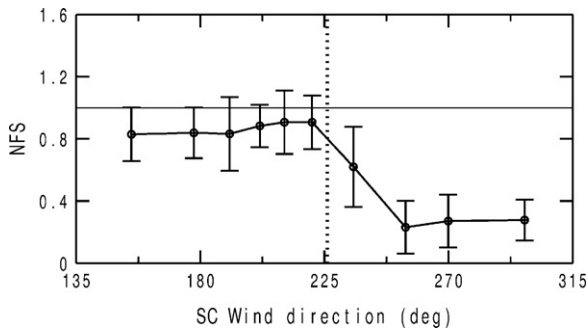


Fig. 9. NFS as a function of the subcanopy (SC) wind direction. The dashed vertical line denotes the critical wind direction using the 95% rule. Error bars denote the 95% confidence interval. Each of the 10 bins contains 53 1-hour average samples.

these three sites the dependence of the subcanopy wind direction on the wind speed or mixing strength above the canopy is very similar to the patterns observed in May–August of 2004 and discussed above. For the strongest wind speeds above the canopy greater than 5 or 6 m s⁻¹, the spatial variation in the subcanopy wind direction approaches zero, and the subcanopy wind direction approaches the wind direction above the canopy.

3.4. Choice of filter

Using the subcanopy wind direction to identify missing CO₂ flags only 40% of the data compared to 70% for u^* , and the average NFS for wind directions less than the critical value of 226° is 0.91 (Fig. 9). The subcanopy wind direction filter is physically more satisfying than filters based on above-canopy variables, but may not work at all sites, for example, where the local drainage flow tends to be in the same direction as the above-canopy flow. In such case, it may not be possible to identify the decoupled flow regime using wind direction alone. Clearly, the critical wind direction will be site-specific.

All the filter variables tested (u^* , σ_w , R_b , z/L and the subcanopy wind direction) work well at this site for identifying missing CO₂. Selecting which filter to use in practise is not obvious. The best filter variable may be site-specific. In terms of maximizing the amount of data retained by the filter, the subcanopy wind direction filter is superior using the 95% rule because it retains twice as much data compared to u^* at this site (Table 1). Maximizing the amount of data retained is important for reducing the uncertainty in developing the temperature and moisture dependencies of the

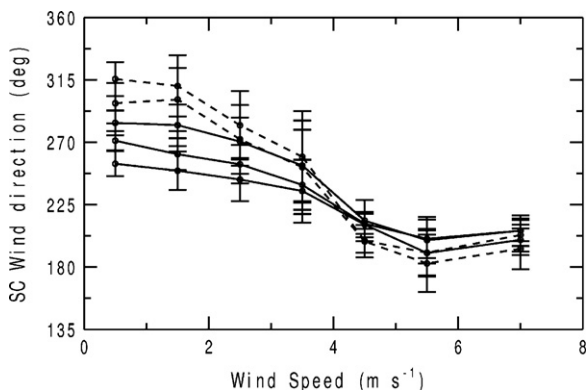


Fig. 10. The subcanopy (SC) wind direction from the five Handar anemometers deployed in 2003 (see text) as a function of the mean wind speed above the canopy. The number of 1-h average data points in the wind speed bins is 122, 72, 81, 58, 33, 14 and 16 for wind speed bins 0–1, 1–2, 2–3, 3–4, 4–5, 5–6 and 6–8 m s⁻¹, respectively. Error bars denote the 95% confidence interval.

retained FS data for developing annual sums of respiration. The friction velocity is desirable because u^* is proportional to the vertical stress divergence, which appears directly in the momentum budget and partially determines if the uncoupled downslope flow regime develops. The bulk Richardson number and z/L are attractive as filter variables because they are dimensionless and thus more general; however, the critical R_b and z/L values will presumably depend on the canopy structure and terrain slopes. Based on the amount of data retained, the z/L filter is slightly superior to the u^* filter at this site (Table 1).

An alternative filtering approach was recently proposed by Van Gorsel et al. (2009). Their method retains the nocturnal FS data only for the particular 3-h period where the 30-day average nocturnal FS is a maximum. Additional conditions are imposed based on stability (z/L) and an estimate of respiration from the light response curve approach (see details in Van Gorsel et al., 2009). Their approach assumes that there are certain periods every night (presumably the same time each night) where advection of CO₂ is negligible, and that these periods can be identified by finding the maximum FS. We find that for some weak-wind nights the inferred advection is significant throughout the entire night, while for some strong wind nights the inferred advection is negligible all night. We also find that the time of onset of drainage flow (and missing CO₂) varies considerably from night to night depending on the wind speed above the canopy.

4. Conclusions

Characteristics of the flow above and below a tall open forest canopy were studied in the context of the missing CO₂ problem, where the eddy-covariance CO₂ flux plus the CO₂ storage term (FS) is significantly less than the coincident chamber-based estimate of ecosystem respiration (ER) in strongly stable nocturnal conditions. Turbulence strength was represented by u^* , σ_w , R_b and z/L . Two nocturnal subcanopy flow regimes were found. Westerly subcanopy downslope flow decoupled from the above canopy flow developed with weak mixing or weak wind above the canopy, and was associated with periods where FS was smaller than ER by up to a factor of 10. This regime supports the hypothesis that in weak wind conditions cold air drainage flow systematically advects air with lower CO₂ concentration to the site, leading to the missing CO₂. The westerly subcanopy downslope flow was also associated with much stronger stability in terms of the temperature stratification and z/L . The second regime was characterized by stronger mixing or stronger wind above the canopy and a southerly subcanopy flow coupled to the above canopy flow, and was not associated with missing CO₂ or surplus CO₂. This regime supports the hypothesis that the advection terms are small compared to FS for strong wind conditions. Estimates of the buoyancy forcing and the vertical stress divergence were consistent with the decoupled and coupled regimes. At this site, the best choice for an above-canopy filter variable to identify the two regimes was z/L based on the amount of data retained by the filter and the average FS/ER of the retained data.

Acknowledgments

We gratefully acknowledge John Wong for field work and the two reviewers for their helpful comments. This research was supported by the Office of Science (BER), U.S. Department of Energy (DOE, Grant DE-FG02-06ER64318).

References

- Acevedo, O.C., Moraes, O.L.L., Degrazia, G.A., Fitzjarrald, D.R., Manzi, A.O., Campos, J.G., 2009. Is friction velocity the most appropriate scale for correcting nocturnal carbon dioxide fluxes? *Agric. Forest Meteorol.* 149, 1–10.
- Aubinet, M., Heinesch, B., Yernaux, M., 2003. Horizontal and vertical CO₂ advection in a sloping forest. *Bound. Layer Meteorol.* 108, 397–417.

- Aubinet, M., coauthors, 2005. Comparing CO₂ storage and advection conditions at night at different Carboneuroflux sites. *Bound. Layer Meteorol.* 116, 63–94.
- Belcher, S.E., Finnigan, J.J., Harman, I.N., 2008. Flows through forest canopies in complex terrain. *Ecol. Appl.* 18, 1436–1453.
- Crill, P.M., 1991. Seasonal patterns of methane uptake and carbon dioxide release by a temperate woodland soil. *Global Biogeochem. Cycles* 5, 319–334.
- Falge, E.M., coauthors, 2001. Gap filling strategies for defensible annual sums of net ecosystem exchange. *Agric. Forest Meteorol.* 107, 43–69.
- Feigenwinter, C., Bernhofer, C., Vogt, R., 2004. The influence of advection on the short term CO₂ budget in and above a forest canopy. *Bound. Layer Meteorol.* 113, 201–224.
- Finnigan, J.J., 1999. A comment on the paper by Lee (1998): on micrometeorological observations of surface-air exchange over tall vegetation. *Agric. Forest Meteorol.* 97, 55–64.
- Finnigan, J.J., Belcher, S.E., 2004. Flow over a hill covered with plant canopy. *Quart. J. Roy. Meteorol. Soc.* 130, 1–29.
- Göckede, M., coauthors, 2008. Quality control of CarboEurope flux data—Part 1: coupling footprint analyses with flux data quality assessment to evaluate sites in forest ecosystems. *Biogeosciences* 5, 433–450.
- Goulden, M.L., Munger, J.W., Fan, S.M., Daube, B.C., Wofsy, S.C., 1996. Measurements of carbon sequestration by long-term eddy covariance: methods and a critical evaluation of accuracy. *Global Change Biol.* 2, 169–182.
- Goulden, M.L., Crill, P.M., 1997. Automated measurements of CO₂ exchange at the moss surface of a black spruce forest. *Tree Physiol.* 17, 537–542.
- Gu, L., Falge, E.M., Boden, T., Baldocchi, D.D., Black, T.A., Saleske, S.R., Suni, T., Verma, S.B., Vesala, T., Wofsy, S.C., Xu, L., 2005. Objective threshold determination for nighttime eddy flux filtering. *Agric. Forest Meteorol.* 128, 179–197.
- Heinesch, B., Yernaux, M., Aubinet, M., 2006. Some methodological questions concerning advection measurements: a case study. *Bound. Layer Meteorol.* 122, 457–478.
- Irvine, J., Law, B.E., 2002. Contrasting soil respiration in young and old-growth ponderosa pine forests. *Global Change Biol.* 8, 1183–1194.
- Irvine, J., Law, B.E., Martin, J., Vickers, D., 2008. Interannual variation in soil CO₂ efflux and the response of root respiration to climate and canopy gas exchange in mature ponderosa pine. *Global Change Biol.* 14, 2848–2859.
- Katul, G.G., Finnigan, J.J., Poggi, D., Leuning, R., Belcher, S.E., 2006. The influence of hilly terrain on canopy atmosphere carbon dioxide exchange. *Bound. Layer Meteorol.* 118, 189–216.
- Kominami, Y., coauthors, 2008. Biometric and eddy-covariance-based estimates of carbon balance for a warm-temperate mixed forest in Japan. *Agric. Forest Meteorol.* 148, 723–737.
- Law, B.E., Ryan, M.G., Anthoni, P.M., 1999. Seasonal and annual respiration of a ponderosa pine ecosystem. *Global Change Biol.* 5, 169–182.
- Lee, X., Massman, W., Law, B.E., 2004. *Handbook of Micrometeorology: A Guide for Surface Flux Measurement and Analysis*. Kluwer Academic Publishers, Boston, p. 250.
- Lee, X., 1998. On micrometeorological observations of surface-air exchange over tall vegetation. *Agric. Forest Meteorol.* 91, 39–49.
- Leuning, R., Zegelin, S.J., Jones, K., Keith, H., Hughes, D., 2008. Measurement of horizontal and vertical advection of CO₂ within a forest canopy. *Agric. Forest Meteorol.* 148, 1777–1797.
- Mahrt, L., Vickers, D., Nakamura, R., Soler, M.R., Sun, J., Burns, S., Lenschow, D.H., 2001. Shallow drainage flows. *Bound. Layer Meteorol.* 101, 243–260.
- Mahrt, L., 2010. Computing turbulent fluxes near the surface: needed improvements. *Agric. Forest Meteorol.* 150, 501–509.
- Massman, W.J., Lee, X., 2002. Eddy covariance flux corrections and uncertainties in long-term studies of carbon and energy exchanges. *Agric. Forest Meteorol.* 113, 121–144.
- Paw U, K.T., Baldocchi, D.D., Meyers, T.P., Wilson, K.B., 2000. Correction of eddy-covariance measurements incorporating both advective effects and density fluxes. *Bound. Layer Meteorol.* 97, 487–511.
- Schwarz, P., Law, B.E., Williams, M., Irvine, J., Kurpius, M., Moore, D., 2004. Climatic versus biotic constraints on carbon and water fluxes in seasonally drought-affected ponderosa pine ecosystems. *Global Biochem. Cycles* 18, GB4007, doi:10.1029/2004GB002234.
- Staebler, R.M., Fitzjarrald, D.R., 2004. Observing subcanopy CO₂ advection. *Agric. Forest Meteorol.* 122, 139–156.
- Staebler, R.M., Fitzjarrald, D.R., 2005. Measuring canopy structure and the kinematics of subcanopy flow in two forests. *J. Appl. Meteorol.* 44, 1161–1179.
- Sun, J., Dejardins, R., Mahrt, L., MacPherson, I., 1998. Transport of carbon dioxide, water vapor and ozone by turbulence and local circulations. *J. Geophys. Res.* 103, 25873–25885.
- Tota, J., Fitzjarrald, D.R., Staebler, R.M., Sakai, R.K., Moraes, O., Acevedo, O.C., Wofsy, S.C., Manzi, A.O., 2008. Amazon rain forest subcanopy flow and the carbon budget: Santarem LBA-ECO site. *J. Geophys. Res.* 113, G00B02, doi:10.1029/2007JG000597.
- Van Gorsel, E., Leuning, R., Cleugh, A., Keith, Heather, Suni, T., 2007. Nocturnal carbon efflux: reconciliation of eddy covariance and chamber measurements using an alternative to the u^* -threshold filtering technique. *Tellus* 59B, 397–403.
- Van Gorsel, E., coauthors, 2009. Estimating nocturnal ecosystem respiration from the vertical turbulent flux and change in storage of CO₂. *Agric. Forest Meteorol.* 149, 1919–1930.
- Vickers, D., Mahrt, L., 2003. The cospectral gap and turbulent flux calculations. *J. Atmos. Oceanic Technol.* 20, 660–672.
- Vickers, D., Mahrt, L., 2006. Contrasting mean vertical motion from tilt correction methods and mass continuity. *Agric. Forest Meteorol.* 138, 93–103.